Conformational Change and Histidine Control of Heme Chemistry in Cytochrome *c* Peroxidase: Resonance Raman Evidence from Leu-52 and Gly-181 Mutants of Cytochrome *c* Peroxidase†

Giulietta Smulevich,*,‡ Mark A. Miller,§ Joseph Kraut,§ and Thomas G. Spiro*,∥

Dipartimento di Chimica, Università di Firenze, Via G. Capponi 9, 50121 Firenze, Italy, Department of Chemistry, University of California, San Diego, La Jolla, California 92093, and Department of Chemistry, Princeton University, Princeton, New Jersey 08544

Received March 6, 1991; Revised Manuscript Received July 10, 1991

ABSTRACT: Resonance Raman (RR) spectra are reported for Fe(III), Fe(II), and Fe(II)CO forms of site-directed mutants of the cytochrome *c* peroxidase variant CCP(MI), cloned in *Escherichia coli*. The Fe(II) form is five-coordinate (5-c) and high-spin at low pH, but it is six-coordinate (6-c) and low-spin at high pH except when the distal His-52 residue is replaced with Leu, showing the sixth ligand to be the His-52 imidazole. Although the Leu-52 mutant stays 5-c, it does undergo an alkaline transition, as revealed by upshifts and broadening of bands assigned to vinyl C=C stretching (1620 cm^{-1}) and C_β-vinyl bending (402 cm^{-1}). Similar changes are seen for CCP(MI) and other mutants. Thus the alkaline transition induces a conformational change that affects the vinyl groups, probably through changes in their orientation, and that permits the His-52 imidazole to bind the Fe. The RR band arising from the stretching of the proximal Fe(II)–imidazole bond contains components at ca. 235 and 245 cm^{-1} for CCP(MI), which are believed to reflect a double well potential for the H-bond between the proximal His-175 imidazole and the Asp-235 carboxylate group. Loss of this H-bond by mutation of Asp-235 to Asn results in the loss of these two bands and their replacement by a single band at 205 cm^{-1}. Although the Fe(II)–imidazole stretching mode cannot be observed in the 6-c alkaline form of the enzyme, the sixth ligand in the alkaline form of CCP(MI) is photolabile, and the status of the Fe(II)–imidazole bond can be determined in the resulting 5-c-photoproduct. For CCP(MI) at alkaline pH, the conformation change induces an increase in the 235/245-cm^{-1} ratio, reflecting a perturbation of the H-bond potential. In the His-52 → Leu mutant, a 205-cm^{-1} band appears along with the 235/245-cm^{-1} doublet at alkaline pH, indicating partial loss of the proximal H-bond due to the distal alteration. The effect of mutations that perturb the H-bonding network that extends from the distal to the proximal side of the heme is more dramatic: at alkaline pH, His-181 → Gly, Arg-48 → Leu, and Trp-51 → Phe mutants show an Fe(II)–imidazole stretching mode at 205 cm^{-1} exclusively, indicating complete loss of the proximal Asp-235–His-175 H-bond. The conformational changes at alkaline pH apparently exert a stress on the Asp-235–His-175 H-bond that is resisted only if the H-bonding network is intact. The alkaline CO adducts of all mutants except Leu-52 have Fe–CO stretching (RR) and C–O stretching (IR) frequencies characteristic of normal complexes with neutral imidazole fifth ligands (form I′), implying the absence of a strong proximal H-bond. At neutral pH the vibrational frequencies reveal two kinds of CO adduct: linear and ligated by imidazolate (form I), and tilted and H-bonded by a distal group, with a weakened proximal bond (form II). CCP(MI) gives only form I, but the Gly-181 mutant gives a mixture of both forms, reflecting a weakening of the Fe–imidazole bond due to the loss of an anchoring H-bond between the His-181 imidazole and a propionate substituent of the heme. The Leu-52 mutant also gives a mixture of two forms, but in this case the pH dependence is very weak, and both forms are seen, though with a slightly altered intensity ratio, at alkaline pH. Thus, loss of the His-52 imidazole uncouples the distal H-bonding from the alkaline conformation change. Absorption spectra of the alkaline Fe(III) forms indicate that imidazole is again the sixth ligand, except for the Leu-52 mutant, which binds hydroxide instead, giving a mixed-spin RR spectrum. Lowering the pH produces a 5-c RR spectrum for the Leu-52 mutant, but a mixed spectrum for the Gly-181 mutant, with contributions from high- and low-spin 6-c as well as 5-c heme. This effect is again attributed to the loss of the anchoring His-181–propionate interaction, which allows the Fe(III) to more readily bind a water molecule. At low pH values, the Leu-52 mutant shows some 6-c high-spin contribution, as does CCP(MI) itself, but this contribution is buffer-dependent, being somewhat greater for acetate than for citrate. The only mutant failing to show a low pH 6-c contribution is Leu-48, suggesting that the Arg-48 side chain plays an obligatory role in the binding of a sixth ligand, either water or a buffer anion. Since the appearance of a 6-c low pH component has been linked to aging of the protein in the case of baker's yeast CCP, it may be that an alteration which increases the Arg-48 mobility is involved. Functional implications of the distal and proximal interactions and of the acid/alkaline conformation change are discussed.

Cytochrome *c* peroxidase (CCP) is a heme protein that catalyzes the reduction of hydroperoxides via electrons from cytochrome *c* (cyt *c*) (Yonetani, 1976). The availability of high-resolution crystal structures (Poulos et al., 1980; Finzel

† This work was supported by NIH Grant GM 33576 (to T.G.S), NATO Grant 86/0453 (to G.S. and T.G.S.), NSF Grant DMB 88-15718 (to J.K.), and a postdoctoral fellowship from Hemoglobin and Blood Protein Training Grant 5 T32 AM07233-11 (to M.A.M.).

* Authors to whom correspondence should be addressed.
‡ Università di Firenze.
§ University of California, San Diego.
∥ Princeton University.

0006-2960/91/0430-9546$02.50/0

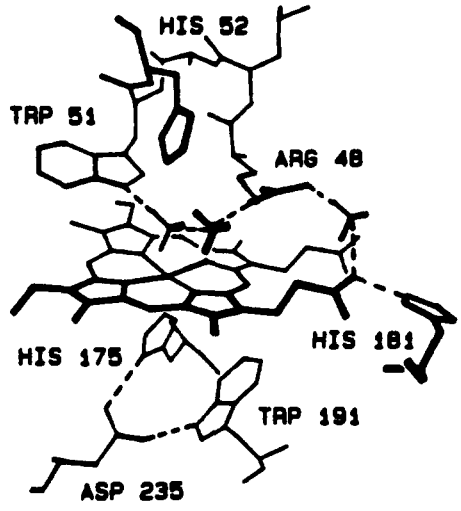

FIGURE 1: Structural diagram of the heme pocket of CCP (Finzel et al., 1984).

et al., 1984; Wang et al., 1990) and of site-directed mutants of cloned protein (Goodin et al., 1986; Fishel et al., 1987) have made CCP an outstanding system for testing the role of heme pocket residues in directing the reactivity of the heme group. We have studied the variant CCP(MI) and a series of its mutants (Smulevich et al., 1988a,b). The suffix MI stands for the extra N-terminal methionine and isoleucine residues that are present in this protein as a result of its expression in *Escherichia coli* bacteria. In addition, the clone selected for CCP(MI) has two residue changes, Asp-152 → Gly and Thr-53 → Ile, relative to the baker's yeast protein (to which the abbreviation CCP refers in the rest of this text). The structure and chemistry of CCP(MI) and CCP are nevertheless very similar (Finzel et al., 1984; Fishel et al., 1987; Scholes et al., 1989; Erman et al., 1990b; Wang et al., 1990; Vitello et al., 1990b).

Resonance Raman (RR) spectroscopy has provided information about key aspects of the heme structure, including the coordination number and spin state, the status of the bond to the proximal imidazole ligand, and of the bonding in the carbon monoxide adduct of the reduced form of the protein. This information for several CCP(MI) mutants has provided a picture of a dynamic interaction between important hydrogen-bond interactions on the proximal and distal side of the heme (Smulevich et al., 1988a,b, 1989a,b; Spiro et al., 1990).

In the present study, we extend this picture significantly with two key mutants: Leu-52 and Gly-181 (see Figure 1 for the location of these residues in the heme pocket). In the first of these, leucine replaces the distal histidine residue, which is believed to play an essential role in the enzyme mechanism as a proton transfer agent (Poulos & Kraut, 1980a). In the second mutant, glycine replaces the His-181 residue, which is thought to be important in the structural stability of the enzyme at alkaline pH as a result of H-bonding between the imidazole side chain and the propionate of heme IV (Finzel et al., 1984); deprotonation of this residue has been implicated in the conformational change observed in the enzyme at alkaline pH (Bosshard et al., 1984; Miller et al., 1990a,b). The RR spectra clarify many aspects of the heme chemistry in both the acid and alkaline conformations. The distal His-52 and Arg-48 residues are shown to form a coupled system for proton transfer and charge stabilization of bound ligands, which is well-suited for peroxide binding and activation. The transition to the alkaline conformation is shown to weaken the proximal and distal H-bonds and to permit coordination of the His-52 imidazole to the heme Fe. This transition is resisted by a chain of H-bonds linking distal and proximal residues, anchored by the His-181–propionate H-bond. It is suggested that the conformational transition might serve to gate the peroxide reaction to the flow of electrons from cyt *c* via modulation of this H-bond in the CCP–cyt *c* complex.

Materials and Methods

The cloning and expression of the gene for yeast cytochrome *c* peroxidase in *E. coli*, as well as the procedures for introduction of single amino acid substitutions by site-directed mutagenesis, have been described (Kaput et al., 1981; Fishel et al., 1987, and references therein). The introduction of the His-181 → Gly mutation into the coding sequence for CCP(MI) has been described previously (Miller et al., 1988). The His-52 → Leu mutation was introduced with a commercially available mutagenesis kit (Amersham). A 25-base oligonucleotide primer obtained from the Peptide/Oligonucleotide Synthesis facility at UCSD with the sequence (5′-CCCAGGTACCTGAAATGAGCCAAGC-3′) was used to convert the CAC (His) codon to CTC (Leu) and introduce a *Kpn*I site through a silent codon change (GGG to GGT) at Gly-55.

Enzymes were isolated from 15–20-L cultures of *E. coli* grown in TB (12 g of bacto-tryptone, 24 g of yeast extract, 10 g of NaCl, 4 mL of glycerol, 3.47 g of KH_2PO_4, and 18.8 g of K_2HPO_4/L) for 36 h at 37 °C. The isolated enzymes were purified and converted completely to the holoenzyme as previously described (Fishel et al., 1987). Purified holoenzymes were recrystallized by exhaustive dialysis against H_2O; the crystalline suspensions were stored in H_2O at −70 °C until use.

Crystals of the enzymes were dissolved in 0.1 M potassium phosphate (pH 6.0). The molar extinction coefficients of the Soret maxima were determined by the pyridine hemochromogen method (Paul et al., 1953) for ferric enzymes in 0.1 M potassium phosphate (pH 6.) at 23 °C. The values obtained under these conditions were CCP(MI,G181), $\epsilon_{408.0}$ = 100 mM^{-1}; CCP(MI,L52), $\epsilon_{405.2}$ = 97 mM^{-1}. The pH dependence of the absorption spectra of ferric enzymes was determined by dilution of enzyme stock solutions of known concentration (in phosphate buffer, pH 6.0) into 1 mL of buffer at the desired pH. The buffers employed for absorption spectra were 0.1 M acetate (pH 5.0), phosphate (pH 6.0–7.5), or Tris (pH 8.0–9.0). Spectra of ferrous and ferrous–CO complexes were determined as follows: a small aliquot (60 μL) of enzyme solution diluted to approximately 0.6 mM (0.1 M potassium phosphate, pH 6.0) was placed in the side arm of a sealed cuvette, and argon (H_2O-saturated) was passed over the sample for 30 min. The sample was then mixed with 2 mL of anaerobic buffer in the cuvette chamber, and the concentration of the ferric enzyme solution was determined from the absorbance at the Soret maximum. The enzyme was reduced to the ferrous state by addition of a small excess of a sodium dithionite solution, and the spectrum was recorded. The sample was converted to the CO complex by flowing CO into the sealed cuvette for 15 min. Absorption spectra were recorded on a Perkin-Elmer Lambda 3b spectrophotometer with thermostated cuvette chambers. Apparent rates of CO dissociation were determined by the oxygen trap method (Wittenberg et al., 1967). The detailed procedure for these experiments has been described elsewhere (Miller et al., 1990b). The CO complex of CCP(MI,L52) was placed in buffer equilibrated with atmospheric oxygen at the required pH. Under these conditions, the CO complex is converted to the ferric enzyme without detectable accumulation of interme-

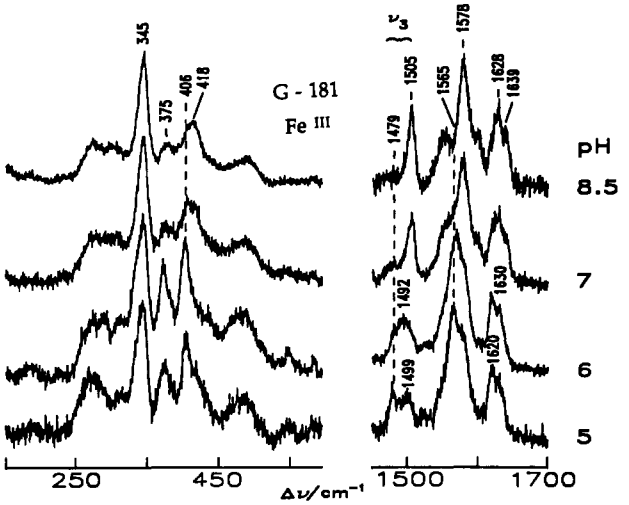

FIGURE 2: Resonance Raman spectra of Fe(III) CCP(MI–Gly-181) at different pH's obtained with 413.1-nm excitation. Conditions: 70-mW laser power at the source, 5-cm^{-1} resolution, 3 and 2 s/0.5 cm^{-1} collection interval for the low- and high-frequency regions, respectively.

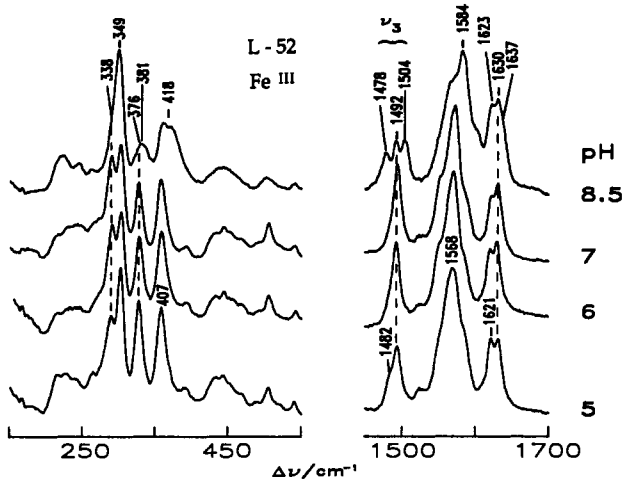

FIGURE 3: Resonance Raman spectra of Fe(III) CCP(MI–Leu-52) at different pH's obtained with 413.1-nm excitation. Conditions: 40-mW laser power at the sample, 5-cm^{-1} resolution, and 10-min collection.

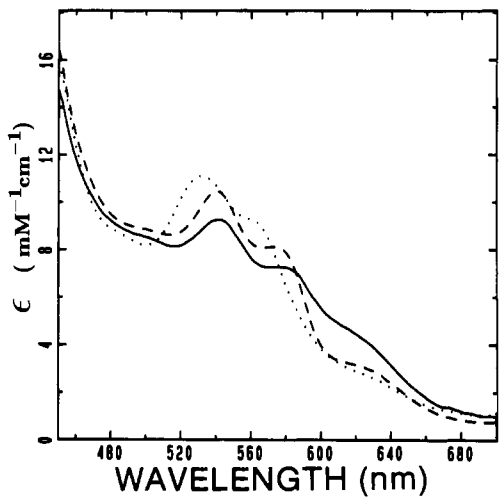

FIGURE 4: Visible absorption spectra of Fe(III) CCP(MI–Leu-52) at pH 8.5 (—) and of CCP(MI–Asn-235) at pH 6 (– – –) and pH 8.5 (···) in the α,β region.

diates. The progress of the reaction was monitored at the wavelength where the maximum difference in absorption between the ferric enzyme and the CO complex was observed. Rate constants for CO dissociation were obtained from linear least-squares analysis of plots of log $(A_0-A_f)/(A_t-A_f)$ versus time over the course of the reaction where A_0 is the initial absorbance at the appropriate wavelength, A_f is the absorbance at infinite time, and A_t is the absorbance at time t.

Crystals of the proteins were dissolved in 0.1 M acetate or citrate (pH 5), phosphate (pH 6–7), MOPS (pH 7), and Tris (pH 8.5 and 9.3) buffers to give protein concentration of 0.2–0.4 mM for RR spectroscopy and 1.5–2.5 mM for IR spectroscopy.

The Fe(II) forms were prepared by adding a minimum volume of dithionite solution to the deoxygenated buffered solutions. At pH 6, the Fe of the Gly-181 mutant was fully reduced within 20 min of adding dithionite. The Fe(II) forms at alkaline pH were prepared by adding degassed buffer and dithionite solutions to the crystals, and the spectra were recorded immediately. The CO adducts were obtained by gently flowing CO (1 atm) (Matheson) from a gas cylinder over the surface of the reduced protein for 20 min. The ^{13}CO (99%) and $C^{18}O$ (98%) adducts were obtained by introducing the gas (Cambridge Isotope Labs) from 0.25- and 0.1-L glass flasks, respectively, to an evacuated NMR tube. The formation of the Leu-52–CO adduct was found to be unusually slow at alkaline pH, requiring 15–20 min to equilibrate. For the IR spectra of the CO adducts, the samples were transferred by a gas-tight syringe flushed with CO to a CaF_2 IR cell (0.1-mm path length) that had been flushed with CO. Buffer solution was used as a reference. The CaF_2 windows permitted UV–vis absorption spectra to be recorded immediately before and after IR spectroscopy to check sample integrity.

The RR spectra were obtained with excitation from the 413.1-nm line of a Kr^+ laser (Coherent), 441.6-nm line of an He/Cd laser (Lyconix), and 457.9-nm line from Ar^+ laser (Coherent). For the Gly-181 mutant, the back-scattered light from a slowly rotating NMR tube was collected and focused into a computer-controlled double monochromator (Spex 1401) equipped with a cooled photomultiplier (RCA) and photon-counting electronics. For the Leu-52 mutant, the scattered light was dispersed with a Spex triplemate monochromator (2400 groove/nm grating) and collected with an optical multichannel analyzer (Princeton Instruments), or (also for Phe-51) the scattered light was collected and focused into a computer-controlled double monochromator (Yobin-Yvon HG2S) equipped with a cooled photomultiplier (RCA) and photon-counting electrons. All the spectra were collected at room temperature.

Infrared spectra were recorded at 25 °C with a Digilab FDS-20C (Gly-181) or a Nicolet 800 (Leu-52) FTIR spectrophotometer.

RESULTS

(A) Fe(III)

His-52 Is the Sixth Ligand at Alkaline pH. All CCP mutants studied to date exhibit an alkaline transition to a low-spin Fe(III) form (Smulevich et al., 1988a). This transition is also seen in the absorption spectrum of the Gly-181 mutant (Miller et al., 1988), whose RR spectra are shown in Figure 2. In the high-frequency skeletal mode region, the ν_3 band is at 1505 cm^{-1}, characteristic of six-coordinate (6-c) low-spin Fe(III) heme, when the pH is adjusted to 7 or 8.5, and the other bands are likewise at the positions expected for this oxidation and spin state (Choi et al., 1983). The behavior of the Leu-52 mutant is quite different, however, as seen in Figure 3. At pH 7, ν_3 and the other high-frequency bands are at frequencies characteristic of five-coordinate (5-c) Fe-

Table I: Absorption Band Maxima (nm) and Millimolar Absorptivities (in Parentheses) of Some Low-Spin Fe(III) Hemoproteins

enzyme	pH	Soret	β	α
Hb-OH (human)[a]	>9	410	540 (11.0)	575 (9.2)
Hb-OH (horse)[b]	>9		540 (9.3)	570 (8.5)
Mb-OH (horse)[c]	>9	411	541 (8.8)	582 (8.7)
HRP-OH[d]	>11	416 (89)	545 (8.6)	572 (6.9)
Asn-235 (–OH)[e,f]	6.0	413.5 (110)	543 (9.6)	579 (7.1, sh)
Leu-52[g]	8.5	413.1 (80)	543 (8.4)	580 (6.4, sh)
CCP, –190 °C[h]	7	416.0 (180)	540 (28)	574 (23, sh)
CCP, 23 °C[h]	8.4	414.0 (95)	532 (9.5)	
CCP, –190 °C[h]	8.4	416.0 (220)	535 (32)	560 (27, sh)
CCP(MI)[i]	9.5	415.0 (100)	534 (10.0)	564 (7.6, sh)
Lys-48[i]	7.8	415.0 (118)	534 (10.1)	563 (8.0, sh)
Leu-48[i]	8.3	414.0 (97)	532 (10.3)	564 (7.5, sh)
Gly-181[j]	8.3	415.0 (98)	534 (9.7)	564 (7.4, sh)
Asn-235[e]	8.5	415.0 (100)	534 (10.0)	563 (8.2, sh)
cyt b_5[k]	5.5	413.0 (113)	532 (10)	560 (9, sh)

[a] Williams (1951). [b] George and Hanania (1953). [c] George and Hanania (1952). [d] Keilin and Hartree (1951). [e] J. M. Mauro, M. A. Miller, and J. Kraut (unpublished observations). [f] Satterlee et al. (1990). [g] Present work. [h] Yonetani et al. (1966). [i] Smulevich et al. (1988a). [j] Miller et al. (1988). [k] Strittmatter and Velick (1956).

(III), while at pH 8.5 there is a mixture of 5-c and of high- and low-spin 6-c Fe(III), reflected in the three distinct ν_3 bands at 1492, 1478, and 1504 cm^{-1}, respectively. Thus, the His-52 mutant is the only one that fails to form a pure low-spin species at alkaline pH.

The absorption spectrum of the alkaline Leu-52 mutant is also unique. Figure 4 shows that at pH 8.5 its α and β bands are at essentially the same positions as those of the Asn-235 mutant at pH 6.0, but they are distinctly red-shifted relative to those of the Asn-235 mutant at pH 8.5. This last spectrum is essentially the same as the alkaline absorption spectra of CCP and of CCP(MI) and all the other mutants studied to date (Smulevich et al., 1988). Their absorption maxima are listed in Table I, where they are seen to be closely matched by those of ferric cytochrome b_5 (Strittmatter & Verlick, 1956), which has histidine residues as fifth *and* sixth ligands. The absorption maxima of alkaline Leu-52 mutant and of the Asn-235 mutant at pH 6.0, on the other hand, resemble those of alkaline met-myoglobin (George & Hanania, 1952) and horseradish peroxidase (HRP) (Keilin & Hartree, 1951) in which the sixth ligand is hydroxide (Asher & Schuster, 1979; Sitter et al., 1988). We conclude from this evidence that the imidazole side chain of His-52 binds the Fe(III) ion at alkaline pH. When this residue is replaced by Leu, hydroxide binds instead. Hydroxide, being a weaker field ligand than imidazole, produces a mixture of spin states, reflected in the 1478- and 1504-cm^{-1} ν_3 bands. The same behavior is seen in met-hemoglobin and met-myoglobin RR spectra (Strekas & Spiro, 1974; Asher & Schuster, 1979). In the Asn-235 mutant, replacement of Asp-235 with Asn disrupts the strong H-bond from the proximal imidazole ligand (His-175), allowing the Fe(III) to bind a distal water molecule (Smulevich et al., 1988a; Wang et al., 1990). This water molecule ionizes with a pK_a between 5 and 6, leaving bound hydroxide, which produces a 6-c mixed-spin heme RR spectrum similar to that seen for the Leu-52 mutant at alkaline pH (Smulevich et al., 1988a). Consistent with this interpretation, Satterlee et al. (1990) find NMR evidence for a hydroxide sixth ligand in the Asn-235 mutant at pH values near 6. (The reported pD was 6.8, but we find empirically a ~0.5 unit pH–pD difference for the absorption spectral change of the Asn-235 mutant). When the pH is raised to 8.5 for the Asn-235 mutant, the bound hydroxide is replaced by the His-52 side chain, as reflected in the absorption maxima (Figure 4 and Table I) and in a pure 6-c low-spin RR spectrum (Smulevich et al., 1988a).

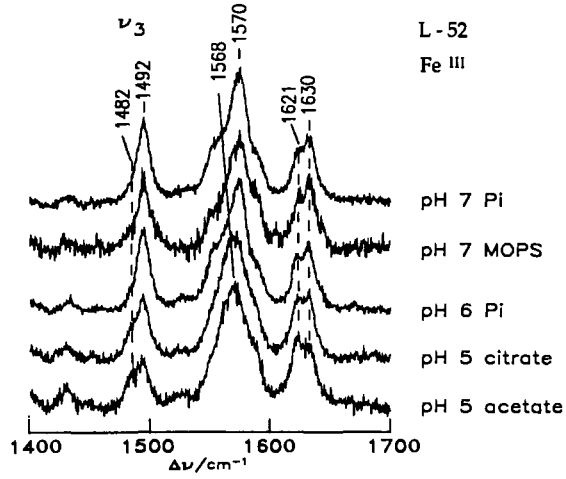

FIGURE 5: Resonance Raman spectra of Fe(III) CCP(MI–Leu-52) in different buffers obtained with 413.1-nm excitation. Conditions are as given in the legend to Figure 2.

Thus CCP and CCP(MI), which contain 5-c Fe(III) heme in neutral solution, undergo an alkaline transition that permits the His-52 side chain to bind to the Fe. In the Asn-235 mutant, however, this transition is preceded by ionization of a bound water molecule, while in the Leu-52 mutant hydroxide binds at alkaline pH in place of the missing His-52 residue.

Water or Anion Binding at Neutral and Low pH. When the pH is lowered from 8.5 to 7, the Leu-52 mutant remains 5-c (Figures 3 and 5), but at pH 5 a ν_3 shoulder at 1482 cm^{-1} indicates the formation of some 6-c high-spin heme. This behavior is the same as that shown by CCP(MI) (Smulevich et al., 1988a). The 6-c population at low pH is a function of the use of acetate buffer; less of it is formed when acetate is replaced by citrate at pH 5 (Figure 5). But even at pH 6 in phosphate, a small 6-c contribution can be seen in the foot of the ν_3 band (Figure 5). We have found some low pH 6-c species in all CCP(MI) mutants studied, except for Leu-48, which shows a pure 5-c ν_3 band at pH values as low as 4.6, even in acetate buffer (Smulevich et al., 1988a). Thus the distal Arg-48 residue appears to be involved in the binding of a distal ligand to the Fe(III) ion at low pH.

The Gly-181 mutant, however, does not show a predominantly 5-c spectrum as the pH is lowered from the alkaline region (Figure 2). At pH 6, ν_3 is very broad and covers the 6-c high- and low-spin, as well as the 5-c, position. At pH 5, the 6-c high- (1479 cm^{-1}) and low- (1499 cm^{-1}) spin components are more clearly resolved. We attribute this behavior to the influence of the H-bond between His-181 and a heme propionate substituent (Figure 1) (Finzel et al., 1984). Since His-181 is connected by a six-residue loop to the proximal His-175, this H-bond has the effect of anchoring the proximal linkage to the heme. When the anchoring H-bond is lost via the Gly-181 substitution, the Fe(III) ion is freer to move into the heme plane and bind a distal water molecule, or hydroxide ion, to form a 6-c mixed-spin complex. Essentially the same behavior was observed for the Phe-191 mutant (Smulevich et al., 1988a). The Trp-191 side chain is H-bonded to the same Asp-235 side chain that accepts the proximal H-bond from the His-175 imidazole. Loss of this anchoring interaction by the Phe-191 substitution likewise permits easier coordination of the heme Fe(III). When the Asp-235 is itself replaced by Asn, in the Asn-235 mutant, the distal coordination is much stronger, and there is no longer any 5-c component present. Thus, the binding of distal water is restrained by the His-175–Asp-235 H-bond, but this interaction is bolstered by the Trp-191–Asp-235 H-bond, as well as the H-bond between His-181 and the heme propionate.

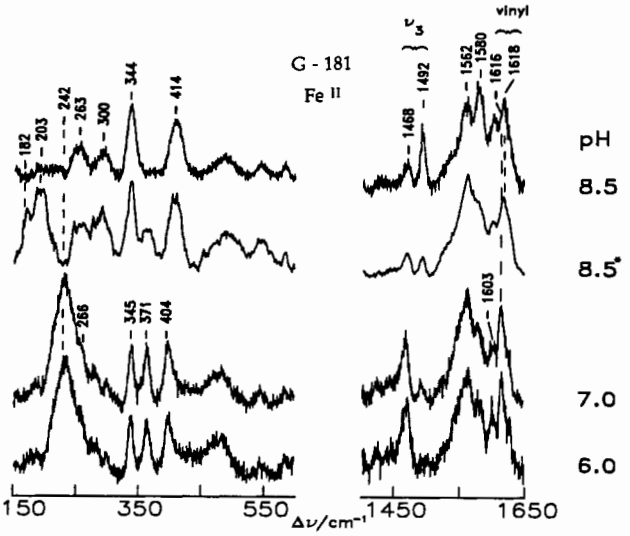

FIGURE 6: Resonance Raman spectra of Fe(II) CCP(MI–Gly-181) at different pH's, obtained with 441.6-nm excitation. Conditions are as given in the legend to Figure 2, except 20-mW laser power at the source. The pH 8.5* refers to a spectrum collected on a stationary sample to induce photolysis, with conditions as given in the legend to Figure 7.

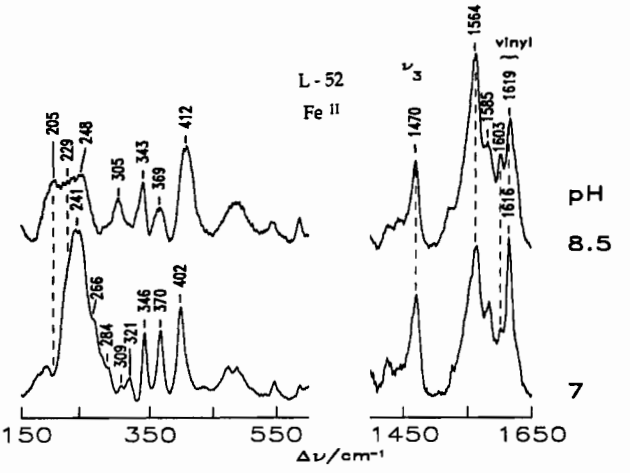

FIGURE 7: Resonance Raman spectra of Fe(II) CCP(MI–Leu-52) at different pH's, obtained with 441.6-nm excitation. Conditions: 25-mW laser power at the source, 5-cm^{-1} resolution, and 20-min collection.

(B) Fe(II)

Proximal H-Bond Breaking at High pH. At neutral and low pH, the reduced form of CCP (Hashimoto et al., 1986; Dasgupta et al., 1989) and of CCP(MI) and all the mutants so far studied (Smulevich et al., 1988a) contain 5-c high-spin Fe(II). The Gly-181 and Leu-52 mutants conform to this pattern as shown by the RR spectra in Figures 6 and 7. The ν_3 band is seen at 1468 and 1470 cm^{-1}, values characteristic of 5-c high-spin Fe(II), and a band appears at 1603 cm^{-1}, which is assignable to ν_{10} in this state (Choi et al., 1983). In the low-frequency region, a strong band appears at ca. 240 cm^{-1}, which is assigned to the stretching of the bond between the Fe(II) and the proximal imidazole side chain of His-175 (Hashimoto et al., 1986). The high frequency of this mode is due to the imidazolate character of the ligand, induced by the strong His-175–Asp-235 H-bond. The Fe–imidazole band is broad and actually contains two components. It has been suggested that they reflect a double well potential for the H-bond, with the proton spending nearly equal time bound to the imidazole and carboxylate anions (Smulevich et al., 1988a). CCP and all the CCP(MI) mutants show this behavior, although there are small variations in the frequencies of the two components (Table II), reflecting perturbations of the H-bond potential by the various heme pocket substitutions. The only exception is the Asn-235 mutant, which shows a narrowed Fe–imidazole band that is strongly shifted to 205 cm^{-1}. This low frequency implies that the proximal H-bond is disrupted when the Asp-235 residue is replaced by Asn (Smulevich et al., 1988a).

Table II: Fe(II)–Imidazole RR Band Frequencies (cm^{-1}) Observed for CCP and Its Mutants

	acid	alkaline
CCP[a]	246/233 sh	233
CCP(MI)[b]	246/233 sh	233
Leu-48[b]	242/227 sh	206
Phe-51[c]	247/229	204
Leu-52[c]	241/229 sh	205/229/248
Gly-181[c]	241/229 sh	203
Asn-235[b]	205	205
Phe-191[b]	246/225	

[a] Hashimoto et al. (1986a). [b] Smulevich et al. (1988a). [c] Present work.

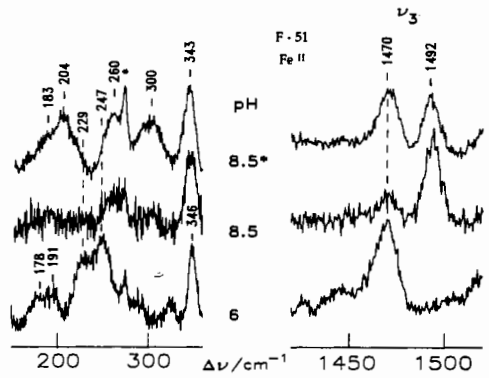

FIGURE 8: Resonance Raman spectra of Fe(II) CCP(MI–Phe-51) at different pH's obtained with 457.9-nm excitation. Conditions: 5-cm^{-1} resolution, 2 s/0.5 cm^{-1} collection interval. Laser power at the sample: pH 6 = 60 mW, pH 8.5 = 10 mW, pH 8.5* = 130 mW. In this latter case, the high power induces photolysis of the CO. An asterisk (*) indicates a plasma line.

At high pH, the RR spectrum of reduced CCP (Hashimoto et al., 1986a) and CCP(MI) (Smulevich et al., 1988a) is likewise that of a 5-c high-spin Fe(II) heme, but the absorption spectrum shows a clear transition to a low-spin form (Conroy et al., 1978; Miller et al., 1990a). This paradox has been shown to result from facile photolysis of the high-pH form in the RR laser beam (Smulevich et al., 1989a). At sufficiently low laser power, a 6-c low-spin RR spectrum can be detected. This photoeffect is illustrated in Figure 6 for the Gly-181 mutant. Two ν_3 bands are seen at the characteristic high- and low-spin frequencies, 1468 and 1492 cm^{-1}. Their intensity ratio is strongly power-dependent, the 1492-cm^{-1} low-spin band nearly disappearing at the higher power level. Figure 8 shows the same effect for another mutant, Phe-51, in which the Trp-51 residue located on the distal side of the heme is replaced by Phe. No photoeffect is seen for the Leu-52 mutant, however (Figure 7). No matter how low the laser power, there was no trace of a low-spin ν_3 band at 1492 cm^{-1}. The absorption spectra of the Leu-52 mutant support this conclusion. The visible region spectra were typical of a 5-c high-spin Fe(II) heme protein between pH 5.0 and 9.0, and no significant changes in this region were observed (Figure 9). Although the Soret band was blue-shifted by approximately 6 nm between pH 7.0 and 8.0 (Figure 9), no further shifts in this peak were observed as the pH was further increased. The present observation strongly supports the view that low-spin Fe(II)

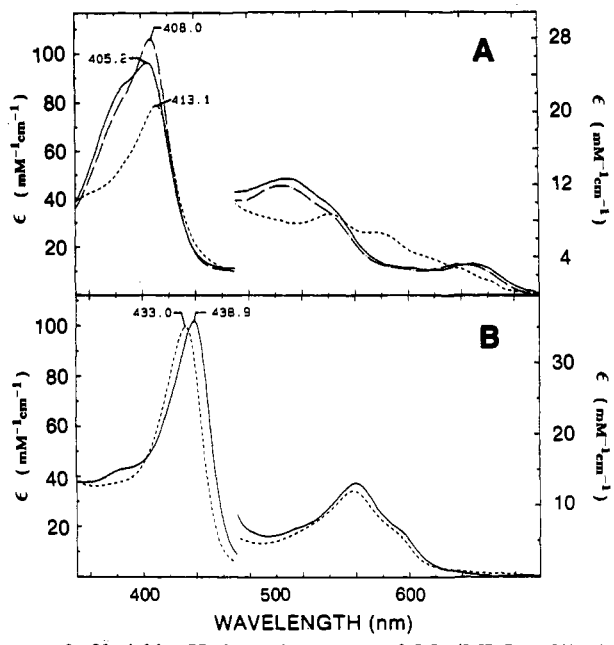

FIGURE 9: Variable pH absorption spectra of CCP(MI-Leu-52). (A) Fe(III), pH 5.0 (---), pH 6.0 (—), and pH 8.5 (···); (B) Fe(II), pH 6.0 (—) and pH 8.5 (···).

formation at high pH is due to the binding of the His-52 imidazole as the sixth ligand.

The low-frequency RR spectrum of photolyzed alkaline Fe(II) CCP (Hashimoto et al., 1986a) and CCP(MI) (Smulevich et al., 1988a) still contains a broad ca. 240-cm^{-1} band, although the lower frequency component (233 cm^{-1}) gains relative intensity, producing an apparent downshift in the band maximum (Dasgupta et al., 1989). Thus, photodissociation of the His-52 ligand leaves a 5-c heme in which the His-175 ligand is still H-bonded to Asp-235, although the H-bond potential is perturbed. In contrast, the Gly-181 mutant (Figure 6) shows a strong band at 203 cm^{-1} when the laser power is high. This is the same frequency as seen for the Fe(II)–Im stretching mode in the Asn-235 mutant at acidic pH, where the proximal H-bond is absent. Thus, the replacement of the His-181 residue by Gly leaves the alkaline photoproduct without a proximal H-bond. We attribute this change to the loss of the anchoring His-181–propionate H-bond. Interestingly, the Phe-51 mutant (Figure 8) also gives a 204-cm^{-1} band when the alkaline Fe(II) form is photolyzed, showing that distal as well as proximal substitutions can perturb the proximal H-bond in the alkaline form. In the case of the Leu-52 mutant (Figure 7), the 5-c high-spin Fe(II) form (for which photolysis is not required) shows a broad and complex Fe–imidazole band, with components at 248 and 229 as well as 205 cm^{-1}. It appears that the proximal H-bond is lost for a fraction of the molecules but retained for the other fraction.

Vinyl Modes Monitor pH-Linked Conformation Change. RR spectra of protoporphyrin complexes contain bands arising from local modes of the vinyl substituents (Choi et al., 1983). The vinyl C=C stretching modes, near 1620 cm^{-1} and the $C_\beta C_1 C_2$ bending modes, near 410 cm^{-1}, stand out clearly. There are two of each of these modes, in- and out-of-phase combinations of the local motions on each of the two vinyl groups. In some heme protein spectra, two bands are seen near 1620 cm^{-1} that are not porphyrin skeletal modes, and Yu and co-workers have definitively assigned the two vinyl C=C stretches in the RR spectrum of an insect hemoglobin using selective deuteration of the two vinyl groups (Gersonde et al., 1989).

The RR spectra of the reduced Leu-52 mutant (Figure 7) give clear evidence for an alkaline transition that affects these vinyl modes. At pH 7, the C=C stretching and $C_\beta C_1 C_2$ bending modes give rise to sharp bands at 1616 and 402 cm^{-1}, but at pH 8.5 they broaden significantly and shift up, to 1619 and 412 cm^{-1}. Thus, it appears that the pair of modes of each type have the same frequency at pH 7, but at pH 8.5 they separate slightly in frequency, and the average frequency increases. An alternative explanation is that only one mode of each pair is subject to resonance enhancement at low pH but that the second mode, which is at slightly higher frequency, becomes enhanced via the alkaline transition. The heme group is 5-c high-spin at both pH values, and there is no change in the high-frequency skeletal modes. Thus, the alkaline transition does not affect the structure of the heme complex but does affect the vinyl groups.

The same effects are seen in the RR spectra of the reduced Gly-181 mutant (Figure 6). The vinyl bands broaden at pH 8.5 and shift up, from 1616 to 1618 cm^{-1}, and from 404 to 414 cm^{-1}. The unphotolyzed fraction of low-spin heme in the alkaline solution complicates the RR spectra, but these changes are clearly detectable. Similar changes can also be seen in published spectra of CCP(MI) and of other mutants (Smulevich et al., 1988a).

Other pH-dependent changes are evident in the low-frequency spectra of the Leu-52 and Gly-181 mutants, aside from the Fe–imidazole band discussed above. The sharp band at 370 cm^{-1}, seen in the neutral solutions, broadens considerably at pH 8.5. A band at this frequency in cytochrome c has been tentatively assigned as a bending mode of the propionate substituents (Hildebrandt et al., 1990a,b). Perceptible broadening is also seen for the 345-cm^{-1} band, which is assigned to ν_8, an in-plane bend of the porphyrin–substituent bonds (Li et al., 1990). The pH 8.5 spectra contain bands at 300 and 305 cm^{-1} for the Gly-181 and Leu-52 mutants, respectively, which disappear at neutral pH and are replaced by multiple weaker bands. The assignment of these bands is uncertain, although out-of-plane deformations of the skeleton are expected in this region (Li et al., 1989).

Similar pH-dependent effects can be seen in the Fe(III) spectra (Figures 2 and 3). The vinyl $C_\beta C_1 C_2$ bends again shift up, from 406 to 418 cm^{-1}, and broaden significantly upon alkalinization; in the case of the Leu-52 mutant, a double band can be seen at pH 8.5. The 375-cm^{-1} band also broadens greatly. The transition pH for these changes is between 7 and 8.5 for the Leu-52 mutant, just as in the reduced form, but between 6 and 7 for Gly-181, significantly lower than the reduced form. We attribute this change in the transition pH to the coordination of the heme Fe ion by the His-52 side chain in the alkaline but not in the acid form. Its binding is expected to be stronger for Fe(III) than for Fe(II), thereby shifting the transition pH to a lower value.

We note also that a currently unassigned band at 337 cm^{-1} shows intensity variations that are pH-dependent, but in a manner that depends on the mutation. For the Leu-52 mutant, its intensity decreases at low pH, while for CCP(MI) and other mutants such as Gly-181 it increases at low pH.

The vinyl C=C assignments are less clear cut for the Fe(III) proteins because of overlap by ν_{10}, which is found at ca. 1640 cm^{-1} for 6-c low-spin complexes and at ca. 1630 cm^{-1} for 5-c high-spin complexes. An additional band seen at 1620 cm^{-1} for both mutants at low pH is attributable to the vinyl C=C stretch. In the Gly-181 mutant a broad band at 1628 cm^{-1} is seen at pH 8.5. This band is not ν_{10}, since there is no 5-c high-spin heme in this species, and it is therefore assigned to vinyl C=C stretching. The same band is seen for the Leu-48,

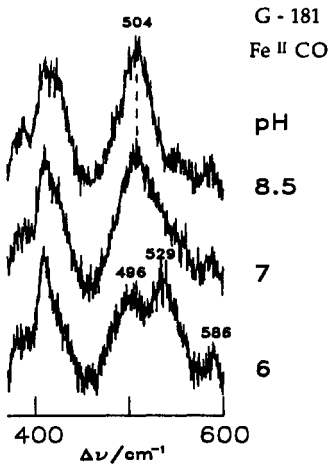

FIGURE 10: Resonance Raman spectra of CCP(MI–Gly-181)-CO at different pH's. Conditions are as given in the legend to Figure 2, except 5 mW laser power at the sample and 5 s/0.5 cm^{-1} collection interval.

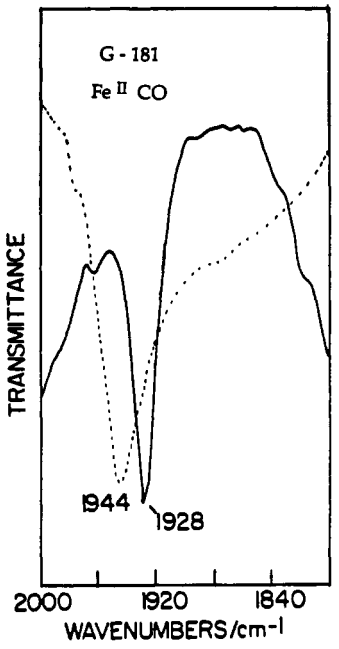

FIGURE 11: IR spectra of CCP(MI–Gly-181)–CO at different pH's [(—) pH 6; (---) pH 8.5]. A total of 128 transients were accumulated; the spectral resolution was 8 cm^{-1}.

Phe-51, and Asn-235 mutants (Smulevich et al., 1988a), all of which are purely low-spin at alkaline pH. This mode also contributes to the 1630-cm^{-1} band of the Leu-52 mutant at pH 8.5 (Figure 2) since a much smaller fraction of the heme is five-coordinate at this pH than at pH 7, where the 1630-cm^{-1} band is about equally strong. It is *not* seen, however, when the low pH forms of CCP and its mutants are converted to the low-spin state by lowering the temperature (Smulevich et al., 1989b, 1990a,b). Thus, the 1628-cm^{-1} band is a second vinyl mode that appears only in the alkaline forms. The separation of the C=C frequencies at high pH is therefore somewhat greater than that seen in the reduced proteins. We note that two vinyl modes at ca. 1620 and 1630 cm^{-1} have also been assigned for Fe(III) HRP (Terner & Reed, 1985).

(C) Fe(II)CO

In CO adducts of heme, the Fe–CO stretching and Fe–C–O bending RR bands are expected at ca. 500 and 580 cm^{-1}, respectively (Kerr & Yu, 1988). The CO adduct bands for the Gly-181 mutant are much like those of CCP itself

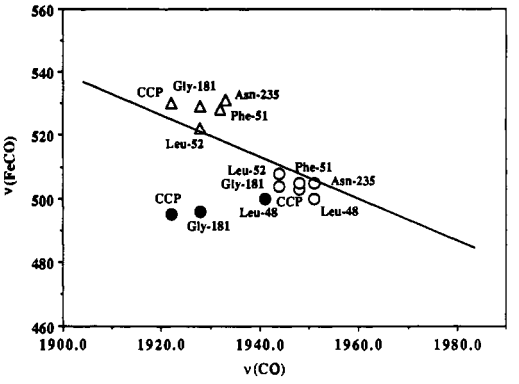

FIGURE 12: Plot of observed ν(FeCO) vs ν(CO) adducts of five mutants together with CCP. The line represents a least-squares fit for a large number of heme CO adducts with imidazole ligands (Li & Spiro, 1988). (○) form I, (△) form II, (●) form I′ (see text).

(Smulevich et al., 1986). As seen in Figure 10, there is a single 504-cm^{-1} Fe–CO band at pH 8.5 but two bands, at 496 and 529 cm^{-1}, when the pH is lowered to 6. These two band shifted to 491 and 522 cm^{-1} when the ^{13}CO adduct was prepared, as expected for Fe–CO modes; the 529-cm^{-1} band was observed to shift farther, to 516 cm^{-1}, when $C^{18}O$ was used (the lower frequency band was obscured in this spectrum). The 586-cm^{-1} Fe–C–O bending mode, identifiable via its sensitivity to ^{13}CO substitution (Tsubaki et al., 1982), shows up at pH 6, while at pH 8.5 a weaker band at slightly lower frequency is attributable to a porphyrin mode. The transition pH is close to 7, since the spectrum at pH 7 is a superposition of the pH 6 and 8.5 spectra. IR spectroscopy (Figure 11) shows a C–O stretching band at 1928 cm^{-1} when the pH is 6 and at 1944 cm^{-1} when the pH is 8.5, frequencies close to those seen for CCP (Iizuka et al., 1985).

This pattern is interpreted by plotting the Fe–CO stretching frequency against the C–O stretching frequency, as shown in Figure 12. The solid line is a least-squares fit to a large body of data from CO adducts of iron–porphyrin complexes and heme proteins, all having imidazole ligands with normal H-bonds, e.g., to a backbone carbonyl group in the case of myoglobin (Uno et al., 1987; Kerr & Yu, 1988; Li & Spiro, 1988). Complexes with ligands that are significantly stronger or weaker donors than neutral imidazole give points falling below or above the lines, respectively (Li & Spiro, 1988). The distribution of points along the line depends on the extent of electron back-donation from the Fe dπ to the CO π^* orbitals (Tsubaki & Ichikura., 1985; Paul et al., 1985; Tsubaki et al., 1986; Uno et al., 1987; Li & Spiro, 1988). ν(Fe–CO) increases while ν(C–O) decreases as back-bonding increases. Interactions of the bound CO with positively charged and/or H-bond donating groups on the distal side of the heme enhance back-donation. Points high on the line, with ν(Fe–CO) > 520 cm^{-1} and ν(C–O) < 1935 cm^{-1}, are believed to reflect distal H-bond interactions (Smulevich et al., 1988b).

The point representing the alkaline Gly-181–CO adduct, called form I′, is at a position characteristic of a normal heme–CO complex, like MbCO (Fuchsman & Appleby, 1979; Ramsden & Spiro, 1989). All the alkaline adducts of CCP and of the CCP(MI) mutants fall in the same region. The two low pH Fe–CO frequencies of Gly-181 give rise to two points, both with the same low C–O frequency. The point with the lower Fe–CO frequency, called form I, falls far below the line and is believed to reflect the imidazolate character of the strongly H-bonded His-175 residue; imidazolate is a stronger donor ligand than is imidazole. The point with the higher Fe–CO frequency, called form II, falls slightly above the line. It is believed to reflect H-bond donation from a distal residue,

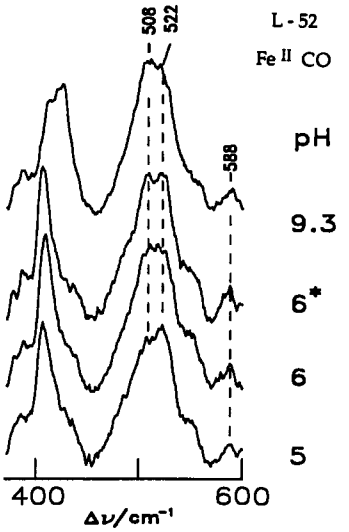

FIGURE 13: Resonance Raman spectra of CCP(MI–Leu-52)-CO at different pH's. Conditions are as given in the legend to Figure 3, except 5-mW laser power at the sample and 20 m in collection. pH 6* refers to a concentration of the protein, 1.5 mM, 5 times higher than the concentration used for the other preparations.

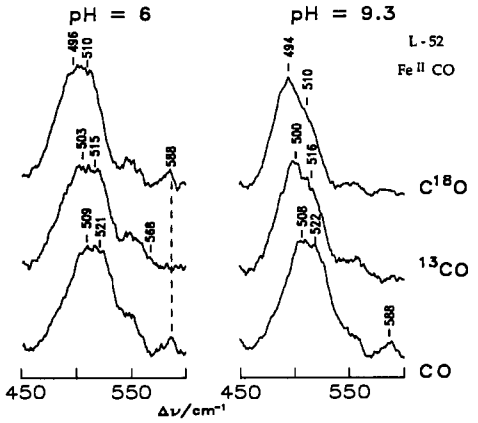

FIGURE 14: Resonance Raman spectra of CCP(MI–Leu-52)-CO and its ^{13}CO and $C^{18}O$ analogues at different pH's. Conditions are as given in the legend to Figure 13.

Arg-48, to the bound CO, together with a weakening of the proximal bond. For CCP, the ratio of form I to form II was found to depend on the CO and protein concentrations, higher CO or lower protein concentrations favoring form II (Smulevich et al., 1986). A similar concentration dependence was observed for the Gly-181 mutant of CCP(MI).

The spectroscopic pattern is quite different for the Leu-52 mutant, as shown in Figures 13 and 14. A doublet Fe–CO stretching band, with components at 508 and 522 cm^{-1}, is seen in the RR spectra at all pH values from 5 to 9.3, but there is a slight shift in the intensity ratio, favoring the 522 cm^{-1} component at low pH. The ratio is insensitive to the protein concentration, as seen by the middle two spectra of Figure 13, obtained at pH 6 for solutions with a 5-fold difference in protein concentration. To ensure that both components really do arise from Fe–CO stretching, we carried out isotopic substitution with ^{13}CO and $C^{18}O$. As seen in Figure 14, both components did shift by the required increments on isotopic substitution. The Fe–C–O bend was also identified at 588 cm^{-1} by its sensitivity to ^{13}CO but not $C^{18}O$ substitution.

The C–O stretching IR band (Figure 15) is also a doublet, with 1944- and 1928-cm^{-1} components. The 1928-cm^{-1} component is favored slightly at low pH, thereby connecting it with the 522-cm^{-1} component of the Fe–CO stretching doublet.

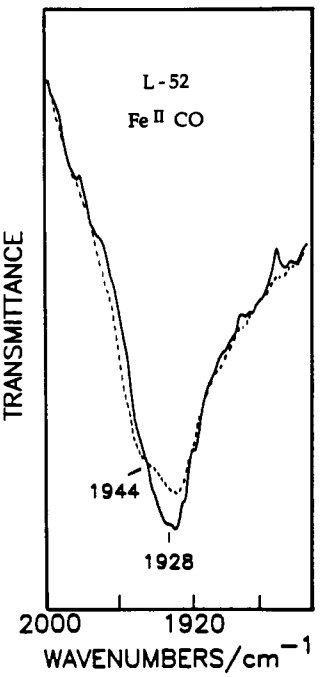

FIGURE 15: IR spectra of CCP(MI–Leu-52)–CO at different pH's [(—) pH 6; (---) pH 9.3]. A total of 128 transients were accumulated; the spectral resolution was 4 cm^{-1}.

When the Leu-52 points are plotted on the diagram in Figure 12, they fall in familiar regions: normal (form I′) for the 508/1944-cm^{-1} components and distal H-bonded (form II) for the 521/1928-cm^{-1} components. What distinguishes Leu-52 from all the other mutants is the very weak pH dependence of the form II/form I′ concentration ratio. The protein *does* undergo an acid–alkaline transition near neutrality, as can be seen in the upshift (406 to 418 cm^{-1}) and broadening of the vinyl $C_\beta C_1 C_2$ bending mode between pH 6 and 9.3 (Figure 11). But this transition is accompanied by only a slight intensity shift from the 522- to the 508-cm^{-1} component, and a comparable shift in the other direction is seen between pH 6 and 5. Thus, the form II/form I′ ratio shows a gradual response to wide pH changes, but it is not responsive to the well-defined acid–alkaline transition of the protein.

(D) pH Dependence of the CO Dissociation Rate in the Leu-52 Mutant

Optical and redox titrations have shown that the acid–alkaline transition in both Fe(II) CCP and its CO adduct represents a cooperative two-proton ionization (Conroy et al., 1978; Iizuka et al., 1985). A similar two-proton ionization has also been reported for the acid–alkaline transition in Fe(II) CCP(MI) and its CO complex (Miller et al., 1990a,b). With the exception of His-181 → Gly, conversion of the mutant Fe(II) and Fe(II)–CO enzymes from acidic to alkaline forms by a cooperative two-proton ionization was detected by optical and/or kinetic data (Miller et al., 1990b). In the case of the Gly-181 mutant, the acid–alkaline transition of both the Fe(II) and the Fe(II)–CO complex indicated a single-proton ionization, thus implicating His-181 as one of the two residues involved in the two-proton ionization.

It has previously been suggested that reduction of Fe(III)CCP to the Fe(II) state results in the protonation of distal His-52 and that the coordination of His-52 to the iron in the acid–alkaline transition of the Fe(II) enzyme results from cooperative deprotonation of His-181 and His-52, (Conroy et al., 1978; Miller et al., 1990a). To test this notion, the pH

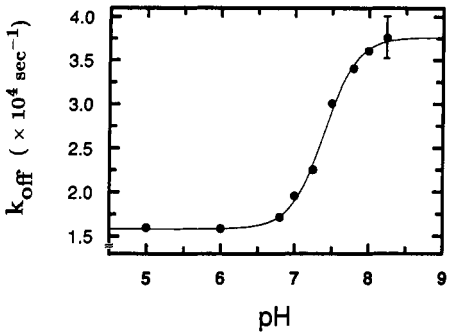

FIGURE 16: pH dependence of CO dissociation rate for CCP(MI–Leu-52). All reactions were in 0.1 M buffers, at 23 °C. Buffers are MES, pH 5.0; phosphate, pH 6.0–7.8; Tris, pH 8.0–8.25. The solid line is the best fit to the data by a nonlinear least-squares program, the parameters of the fit line are $k_a = 1.58 + 0.04 \times 10^{-4}$ s^{-1}; $K_b = 3.76 + 0.07 \times 10^{-4}$ s^{-1}; $n = 1.94 + 0.27$; $pK_a = 7.40 + 0.03$. The brackets on the pH 8.25 point indicate the error in this point ($n = 4$). The error in the other points is within the size of the dot.

dependence of the CO dissociation rate was examined in the Leu-52 mutant. This parameter is a useful monitor of the acid–alkaline transition in CCP(MI) and all mutants previously examined (Miller et al., 1990b). The results in Figure 16 show that the rate of CO dissociation increased from 1.59×10^{-4} s^{-1} at pH 6.0 to 3.75×10^{-4} s^{-1} at pH 8.25. The observed rates differ by only approximately 2-fold from the dissociation rates observed previously for the acidic (0.7×10^{-4} M^{-1} s^{-1}) and alkaline (8.0×10^{-4} M^{-1} s^{-1}) forms of Fe(II)–CO CCP(MI) (Miller et al., 1990b), consistent with a small influence of the distal His on the rate of CO dissociation. The best fit of the data indicates conversion between two enzyme forms by a cooperative two-proton ionization, with an apparent $pK_a = 7.4$. The most straightforward interpretation of this result is that the His-52 residue does *not* titrate in the acid–alkaline transition of the Fe(II)–CO complex of CCP(MI). It cannot be entirely excluded that it does titrate but that the His-52 → Leu replacement somehow alters the pK_a of another residue, causing it to titrate at pH 7.4 in place of His-52. This would be an unlikely coincidence, however.

Discussion

(A) Implications for Enzyme Activity

How do the interlocking distal and proximal interactions affect the function of CCP? The proposed mechanism of the peroxidase reaction is diagrammed in Figure 17. The enzyme in its unligated Fe(III) form reacts with hydroperoxides to form the intermediate compound I (Yonetani, 1976), which is reduced back to the native protein by two electrons. Compound I contains ferryl [Fe(IV)=O] heme and an organic radical, which has recently been identified, via mutagenesis, EPR, and ENDOR spectroscopy, as the radical cation of the Trp-191 indole ring (Scholes et al., 1989; Sivaraja et al., 1989). This side chain is located on the proximal side of the heme and is H-bonded, along with His-175, to the Asp-235 side chain (Figure 1). Consistent with this assignment, the Phe-191 mutant transiently forms a compound I with a radical on the porphyrin ring, as in the case of HRP (Erman et al., 1989).

The initial product of the reaction with hydroperoxides is proposed to be the complex shown in brackets, which breaks down rapidly to compound I via heterolytic cleavage of the O–O bond and release of ROH. This complex has not been detected, but van Wart and co-workers report low-temperature spectroscopic evidence for an intermediate preceding the compound I of HRP (Baek & van Wart, 1990); their

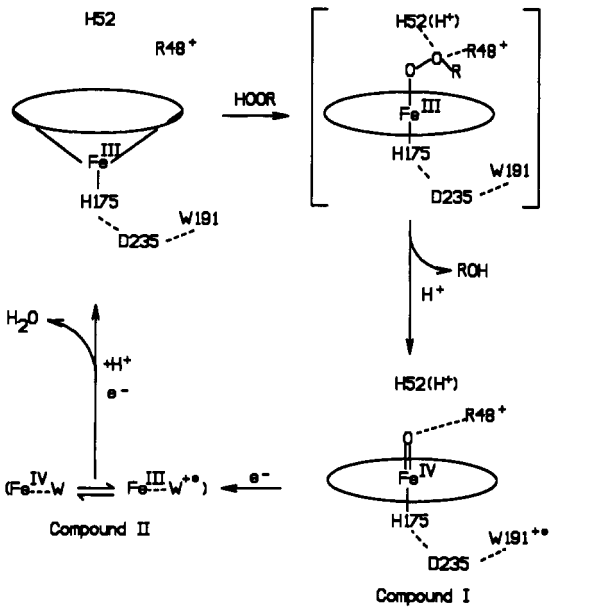

FIGURE 17: Scheme of the proposed mechanism of the peroxidase reaction for CCP.

"compound 0" may be analogous to the proposed CCP complex.

Hydroperoxides also react with hemoglobin and myoglobin, but the rate is some five orders of magnitude slower than the reaction with peroxidases (Dalziel & O'Brien, 1954; George & Irvine, 1956; Loo & Erman, 1975), even though both classes of enzyme contain protoheme bound to a histidine proximal ligand and have a distal histidine near the exogenous ligand-binding site. What mainly distinguishes peroxidase and globin active sites is the presence in peroxidases of an arginine residue in the binding region and of a strong hydrogen bond from the proximal imidazole to a nearby acceptor side chain. Both factors are expected to accelerate the peroxidase reaction cycle.

Ligand Stabilization by Arg-48 Is Coupled with His-52 Protonation. The Arg-48 residue of CCP is strategically placed to facilitate heterolysis of the O–O bond by stabilizing the developing charge on the RO^- leaving group, as pointed out by Poulos and Kraut (1980a) in their discussion of the mechanism based on the original crystal structure (Poulos et al., 1980). They also proposed that the His-52 residue facilitates proton transfer from the inner to the outer O atom, allowing it to leave as ROH. They were able to build the peroxide complex into the CCP structure, with Arg-48 and His-52 interactions as shown in Figure 17.

The proposed mechanism requires that the imidazole side chain of His-52 is unprotonated in the ligand free enzyme, allowing it to accept the proton from hydroperoxide as the latter binds to Fe. One role for Arg-48 in the active site is to depress protonation of His-52, by virtue of the proximity of the positive charge of the guanidinium group to the imidazole side chain. The finding that His-52 is not involved in the acid–alkaline transition of the Fe(II)–CO complex is consistent with this suggestion. An apparent $pK_a = 5.5$ has frequently been suggested for this residue (Vitello et al., 1990a; Dasgupta et al., 1989). This is the pK_a for loss of peroxidase activity when measured in nitrate-containing buffers (Vitello et al., 1990a; Erman et al., 1974a,b). In phosphate buffer, however, the activity is constant down to pH 4.5 (Balny et al., 1987; Vitello et al., 1990a), indicating that the His-52 pK_a is elevated by specific binding of nitrate ion. Consistent with this inference is the finding that the pK_a for activity loss in nitrate is lowered from 5.5 to 4.0 when the salt concentration

is lowered from 0.1 to 0.001 (Loo & Erman, 1975). Specific effects for other anions are likely.

There has been some confusion over the His-52 pK_a because of the suggestion (Dasgupta et al., 1989) that His-52 protonation results in the appearance of a 6-c high-spin heme in the baker's yeast enzyme. Vitello et al. (1990b) report, however, that the 620/647-nm absorptivity ratio, which reflects the heme coordination state, remains unchanged between pH 4 and 7 in acetate buffer, although the 408/380-nm absorptivity ratio did show an inflection at pH 5.4. This observation suggests that His-52 protonation need not induce binding of a sixth ligand. Conversely, the protonated distal histidine is obviously not *required* for ligand binding, since the Leu-52 mutant also shows an increasing fraction of 6-c high-spin heme at low pH (Figures 5 and 9). CCP(MI) and all previously characterized mutants show 6-c high-spin populations at low pH, with the single exception of the Leu-48 mutant (Smulevich et al., 1988a). No 6-c population was detectable for this mutant down to pH 4.6 in acetate buffer, indicating that the Arg-48 residue is required for water or buffer anion binding. Anni and Yonetani (1987) found that the low-pH 6-c fraction in baker's yeast CCP is undetectable in fresh protein and is associated with aging. The alteration in protein structure that is implied by this observation is suggested to result in increased mobility of the Arg-48 side chain.

A second requirement of the proposed mechanism is the protonation of His-52 accompanying coordination of the peroxy anion. The interaction of Arg-48 with an anionic ligand must therefore increase the apparent pK_a for His-52, permitting proton transfer from ROOH to His-52. La Mar et al. (1988) have shown by NMR that the protonation of the distal His of HRP accompanies cyanide binding, and this residue does not titrate up to pH 11 in the CN adduct. An analogous effect in CCP is consistent with reports that fluoride and cyanide are bound as HF and HCN (Erman, 1974a,b), which is equivalent to simultaneous binding of the anion to the Fe and the proton to His-52 in the active site.

Although the peroxide proton is apparently transferred from His-52 to the ROH heterolysis product, His-52 may be reprotonated from the medium at this stage, by virtue of the interaction of Arg-48 with the remaining peroxide O atom (having a formal −2 charge) (Edwards et al., 1987). The reprotonation is indicated by the uptake of a single proton at neutral pH, while no protons are taken up when an apparent pK_a = 5.4 group is protonated (Loo & Erman, 1975; Conroy & Erman, 1978). The remaining proton required in the overall peroxide reaction is divided between the first and second reduction steps (Conroy & Erman, 1978), consistent with compound II being an equilibrium mixture of ferryl heme and ferric heme plus organic radical (Coulson et al., 1971; Yonetani, 1976). The second proton is taken up when Fe(IV)=O is reduced to Fe(III)–OH, after which the His-52-bound proton is transferred to the departing OH^- ligand, returning His-52 to its unprotonated state.

Modulation of Proximal Donor Strength. There are two ways in which the proximal His-175–Asp-235 H-bond could accelerate the peroxidase reaction: (1) It makes the imidazole ligand a stronger donor and should therefore assist heterolysis of the O–O bond by stabilizing the Fe(IV)=O intermediate. The enhanced electron donation from the imidazolate ligand makes it easier to achieve the Fe(IV) oxidation state. (2) It should promote dissociation of the second product, water, again by making the imidazole ligand a stronger donor and also by exerting a mechanical force on the Fe atom toward a proximal displacement from the heme plane. When the proximal H-bond is lost, as in the Asn-235 mutant, water is stably bound to the Fe(III) form, and it ionizes to hydroxide at relatively low pH (5–6). Preliminary evidence indicates, however, that the Asn-235 reacts with peroxide to form a relatively stable compound I at a rate comparable to that of the native enzyme (J. E. Erman, personal communication). This result seems to imply that, contrary to intuition, the imidazole donor strength does not affect the rate-determining step in the peroxide reaction.

The proximal H-bond is important for the electron transfer steps from cyt *c* via the Trp-191 radical of compound I. In the Asp-235 mutant, whose compound I is reduced only slowly (Miller and Kraut, unpublished observations), the Trp-191 indole ring is flipped relative to its conformation in CCP(MI) (Wang et al., 1990). Clearly, the His-175/Asp-235 interaction plays a key structural role in maintaining the Trp-191 orientation. This role does not extend to HRP, however, for which electrons are transferred directly to the porphyrin ring from substrates that bind near the heme edge. Yet HRP and other plant peroxidases do have strong proximal H-bonds (Teraoka & Kitagawa, 1981; Kimura et al., 1981; Teraoka et al., 1983; Hashimoto et al., 1986), suggesting a universal role in the peroxidase mechanism. We note that relatively low Fe=O stretching frequency in HRP compound I of HRP (Sitter et al., 1986; Hashimoto et al., 1986b) is consistent with the strong proximal H-bond being maintained (Su et al., 1988) in the peroxide reaction.

It is of interest in this connection to note the coupling between the distal residues and the proximal H-bond that is revealed by the properties of the Fe(II) CO adducts. At pH values below the acid–alkaline conformation change, CCP gives a mixture of two adducts, form I and form II. Form I adducts have strong donor fifth ligands and upright non-H-bonded FeCO units, while form II adducts have weak donor fifth ligands and tilted H-bonded FeCO units (Smulevich et al., 1986). These characteristics indicate that the structural requirements for distal H-bonding are incompatible with the maintenance of a strong proximal ligand interaction. The CO adduct of the Leu-52 mutant, however, is a mixture of form II and form I′, not form I. Form I′ has no distal H-bond, but the proximal imidazole donor strength is normal, not imidazolate-like. Thus, the proximal H-bond seems to be weakened in Leu-52 CO adduct, even in the absence of distal H-bonding. The Leu-48 mutant does give rise to a form I adduct (form II cannot arise since the distal H-bond donor Arg-48 is absent) (Smulevich et al., 1988b), but its point on the ν(Fe–CO)/ν(C–O) correlation (Figure 12) is distinctly closer to the normal imidazole line than the other form I adducts, again implying a weakening of the proximal H-bond. Thus, replacement of either His-52 or Arg-48 by Leu appears to weaken the proximal H-bond when the CO adduct is formed. The architecture of the native protein seems to maintain a mechanical coupling between the important distal and proximal residues.

(B) Acid–Alkaline Conformation Change

While many aspects of the heme chemistry of CCP and of CCP(MI) and its mutants change when the pH is raised above neutrality, the present study provides the first evidence that a change occurs which is *independent of the heme ligation.* This evidence is provided by the RR bands associated with the heme vinyl groups, which show a consistent pattern of frequency and/or intensity changes, regardless of alterations in the heme ligands brought about by residue substitutions. This pattern is seen most clearly in the Fe(II) form of the Leu-52 mutant, in which the five-coordination state of the heme is *unaltered* by the acid–alkaline transition. Since the porphyrin skeletal modes are unaffected, the vinyl mode

changes must reflect structural influences on the vinyl substituents themselves. The likeliest explanation is rotation of the vinyl groups with respect to the porphyrin plane, since the rotation angle is expected to influence the extent of vibrational and electronic coupling of the vinyl groups with the ring. It cannot be excluded, however, that changes of the local electric field at the vinyl groups, due to charged and polar residues or to helix dipoles, could produce the spectral changes. The band broadenings and upshifts might result from activation of the second vinyl mode of each type, due to lowering of the effective local symmetry rather than to shifts in the frequencies per se.

Although the vinyl mode changes are seen most clearly for the Fe(II) form of the Leu-52 mutant, they are also evident for the Gly-181 mutant, despite the extra spectral complications associated with the His-52 ligation at high pH. Similar changes are detectable for the Fe(III) forms as well. Reexamination of published spectra of CCP(MI) and various mutants (Smulevich et al., 1988a) reveals the same vinyl mode changes. We infer that these changes reflect an acid/alkaline conformation change of the protein that, among other things, alters the interactions of the vinyl groups with the nearby protein residues. Clear evidence for an altered protein conformation also comes from NMR spectroscopy, since raising the pH of CCP to about 9.5 introduces a new set of heme resonances, which replace those seen below pH 8.5 (Satterlee & Erman, 1983). The available crystal structures of CCP (Poulos et al., 1980; Finzel et al., 1984) and its mutants (Wang et al., 1990) were all obtained from crystals grown from neutral solutions and probably represent the acid conformation. It will be very interesting to analyze the structure of a crystal grown from alkaline solution.

This conformation change is associated with the titration of two protonatable groups in the Fe(II) forms, as revealed by the pH dependence of the absorption spectra, CO rebinding rates, and CO dissociation rates (Iizuka et al., 1985; Miller et al., 1990a,b). His-181 is clearly implicated as one of the protonatable groups, since the number of protons involved in the transition is reduced from two to one in the Gly-181 mutant (Miller et al., 1990a,b). The His-181 residue is H-bonded to a heme propionate group (Figure 1). Presumably the imidazole side chain is protonated in the available crystal structures, and deprotonation would be expected to weaken or break the H-bond. (The propionate might still interact with the remaining proton of neutral imidazole, but this interaction would clearly be weaker than with the imidazolium cation.) This loosening of the H-bond is apparently linked to a larger scale protein conformation change.

The second protonatable group could be another histidine residue, or it could be an amine (Lys) or carboxylate (Asp, Gly) side chain that becomes buried or unburied, respectively, as a result of the conformation change. The second group is probably *not* His-52, since the Leu-52 mutant retains a two-proton titration, and, as noted above, it would be an unlikely coincidence for the substitution to produce an exactly compensating change in pK_a for some other group. In any event, His-52 is believed to be unprotonated above pH ca. 5.5 (unless an anion is bound to the heme) because of the influence of Arg-48, as discussed in the preceding section.

Nevertheless, the acid/alkaline transition does permit binding of the heme Fe by His-52. The absorption spectra of the alkaline low-spin forms are consistent with imidazole, rather than hydroxide, binding to Fe(III), while hydroxide is not a viable alternative for Fe(II). Moreover, the low-spin Fe(II) forms are photolabile, implying an unusually slow rebinding rate for one of the ligands (Jongeward et al., 1988); this phenomenon is plausibly explained in terms of protein-induced strain (Smulevich et al., 1989a). The His-52 imidazole ring is ca. 5 Å distant from the Fe in the available crystal structures, and coordination to the Fe requires a significant backbone displacement. The ligation of the alkaline form therefore reinforces the view that the acid/alkaline transition involves a substantial rearrangement of the protein structure.

Additional evidence for a protein conformation effect on the heme ligation comes from the CO adducts, which are all form I′ at alkaline pH (Smulevich et al., 1988b). The only exception is the Leu-52 mutant, which shows a mixture of form II and I′, at alkaline as well as acidic pH. Form II adducts have a distal H-bond while form I′ adducts do not. The H-bond is donated by the Arg-48 side chain; the crystal structure for the CO adduct of baker's yeast CCP, prepared under conditions (saturated CO) favoring form II, shows a water molecule favorably positioned to form an H-bond relay to the O atom from the Arg-48 side chain (Edwards & Poulos, 1990). Thus, the fact that form II is not seen at alkaline pH *except* in the case of the Leu-52 mutant implies that the His-52 inhibits the interaction of the Arg-48 side chain with the bound CO in the alkaline conformation.

Since the form I′ adducts show proximal ligand donor strengths that are typical of normal imidazole, rather than imidazolate, it is also evident that the *proximal* H-bond is weakened in the alkaline conformation, at least in the CO adducts. This weakening is also evident in the 205-cm^{-1} Fe–imidazole stretching frequency seen in the alkaline pH Fe(II) photolysis product of several mutants, namely, Gly-181, Arg-48, and Phe-51. The residues replaced in these mutants, His-181, Leu-48, and Trp-51, are all connected by an H-bond network, which is diagrammed in Figure 1. In the CCP crystal structure, two water molecules on the distal side of the heme (but not coordinated to the Fe) are held by H-bonds between the side chains of Trp-151 and Arg-48 (Finzel et al., 1984). The latter is also H-bonded to another water molecule, which donates an H-bond to a propionate substituent of the heme. The same propionate accepts another H-bond from the imidazole side chain of His-181, which is connected by a five-residue loop to His-175. Since the Fe–imidazole frequency remains at an elevated value (albeit somewhat shifted from the frequency in the acid conformation) for the alkaline photolysis product of CCP(MI) and baker's yeast CCP, we infer that the entire H-bond chain must be intact for the His-175–Asp-235 H-bond to be preserved in the alkaline form. If any of the three residues in the chain is replaced, the proximal H-bond is lost. Interestingly, the Leu-52 mutant shows Fe–imidazole modes at 205 cm^{-1} as well as 229 and 248 cm^{-1}. Thus, replacing the distal His-52 produces an equilibrium between H-bonded and non-H-bonded His-175. The His-52 residue evidently plays a buttressing role with respect to the proximal H-bond.

Further evidence for the importance of the H-bond chain comes from the variation of the acid/alkaline transition pH on amino acid substitutions. The apparent pK_a is 8.0 for the Fe(II) form of CCP(MI) but is lowered to 7.6, 7.3, and 7.2 for the Asn-235, Gly-181, and Leu-48 mutants, respectively (Miller et al., 1990). Similar effects are apparent in the Fe(III) forms. CCP and CCP(MI) are completely converted to low-spin states only at or above pH 9.0, where the protein is no longer stable. But the mutants with residue replacements in the H-bond chain convert completely to low-spin states at pH values between 7 and 8.5 (Smulevich et al., 1988a). Thus, disruption of the H-bond chain lowers the resistance of the protein to the acid/alkaline switch as the pH is raised. Previous work has shown that the formation of the low-spin al-

kaline form of CCP is complex, and the apparent pK_a observed by conventional spectrophotometric techniques is influenced strongly by the pH-dependent rate of formation of several intermediates (Dhaliwal & Erman, 1985). The decrease in the apparent pK_a of the mutants may represent the effect of loss of the distal H-bonding network on the rate of formation of one or more intermediate states, rather than a specific effect on the apparent pK_a of a single residue.

This behavior may provide a clue to the functional significance of the alkaline conformation. It is notable that His-181 is at the protein surface that is thought to be the site of cytochrome *c* docking (Poulos & Kraut, 1980b; Poulos & Finzel, 1984). Conceivably the binding of cyt *c* could perturb the His-181 H-bond to the heme propionate, thereby lowering the transition pK_a for the alkaline conformation. Preliminary RR evidence that binding of Fe(III) cyt *c* increases the low-spin fraction of Fe(III) CCP is consistent with this hypothesis.[1] If the proposed interaction with His-181 is modulated by the redox state of the bound cyt *c*, then the acid/alkaline conformation change could serve to gate the peroxide reaction via the physiological redox level. This mechanism could serve to protect the protein against peroxide when electrons are unavailable from cyt *c*. It is known that CCP and CCP(MI) lose peroxide reactivity in concert with the transition to the low-spin state at high pH (Vitello et al., 1990b). Thus, it will be very interesting to monitor the CCP conformation in its complex with Fe(II) as well as Fe(III) cyt *c*, with the vinyl RR bands as a probe.

Conclusions

(1) CCP as well as CCP(MI) and all the mutants so far examined undergo an acid/alkaline transition that is manifested by apparent upshifts and broadenings of the vinyl stretching and bending RR bands in the alkaline forms. This conformation change is *independent* of the heme oxidation and ligation state, but it controls the heme chemistry by (a) permitting the His-52 side chain to bind as a sixth ligand, despite its being ca. 5 Å from the Fe in the acid conformation, (b) eliminating the Arg-48 interaction with exogenous ligand, at least in the case of CO, and (c) weakening the proximal His-175–Asp-235 H-bond. This last effect is especially marked when residues in the Trp-51–Arg-48–heme propionate–His-181 H-bond chain are replaced. Such replacement also lowers the acid–alkaline transition pK_a. His-181 is one of the two protonatable groups involved in this transition; the other is unknown, but it is probably *not* His-52. The involvement of His-181 suggests the possibility that the transition might function as a gating mechanism for the peroxide reaction, coupled to electron transfer from cyt *c*.

(2) The His-52 side-chain is *not* protonated at neutral pH; its pK_a is depressed by the electrostatic interaction of the nearby Arg-48 side chain and is probably ca. 5.4 (in nitrate-containing buffers), the transition pH for the inhibition of the peroxide reaction and of anion binding, although the pK_a is ionic strength dependent, consistent with an electrostatic effect. Coordinated anions interact with Arg-48 and raise the His-52 pK_a. His-52 is therefore protonated in concert with anion binding. These coupled electrostatic effects are critical for the enzymatic mechanism; they promote peroxide heterolysis by stabilizing the developing negative charge on the OR^- leaving group and facilitating proton transfer to it via His-52.

(3) The distal His-52 and Arg-48 residues also help in maintaining the His-175–Asn-235 proximal H-bond.

[1] P. Hildebrant, A. M. English, and G. Smulevich (manuscript in preparation).

References

Asher, S. A., & Schuster, T. M. (1979) *Biochemistry 18*, 5377–5387.

Baek, H. K., & van Wart, H. E. (1990) *Biochemistry 28*, 5714–5719.

Balny, C., Anni, H. S., & Yonetani, T. (1987) *FEBS Lett. 221*, 349–354.

Bosshard, H. R., Banziger, J., Hasler, T., & Poulos, T. L. (1984) *J. Biol. Chem. 259*, 5683–5690.

Choi, S., Lee, J. J., Wei, Y. H., & Spiro, T. G. (1983) *J. Am. Chem. Soc. 105*, 3692–3707.

Conroy, C. W., & Erman, J. E. (1978) *Biochim. Biophys. Acta 527*, 370–378.

Conroy, C. W., Tyma, P., Daum, P. H., & Erman, J. E. (1978) *Biochim. Biophys. Acta 537*, 62–69.

Coulson, A. F. W., Erman, J. E., & Yonetani, T. (1971) *J. Biol. Chem. 246*, 917–924.

Dalziel, K., & O'Brien, J. R. P. (1954) *Biochem. J. 56*, 648–659.

Dasgupta, S., Rousseau, D., Anni, H., & Yonetani, T. (1989) *J. Biol. Chem. 264*, 654–662.

Dhaliwal, B. K., & Erman, J. E. (1985) *Biochim. Biophys. Acta 832*, 174–182.

Edwards, S. L., & Poulos, T. L. (1990) *J. Biol. Chem. 265*, 2588–2595.

Edwards, S. L., Poulos, T. L., & Kraut, J. (1984) *J. Biol. Chem. 259*, 12984–12988.

Edwards, S. L., Xuong, N. H., Hamlin, R. C., & Kraut, J. (1987) *Biochemistry 26*, 1503–1511.

Erman, J. E. (1974a) *Biochemistry 14*, 34–39.

Erman, J. E. (1974b) *Biochemistry 14*, 39–44.

Erman, J. E., Vitello, L. B., Mauro, J. M., & Kraut, J. (1989) *Biochemistry 28*, 7992–7995.

Finzel, B. C., Poulos, T. L., & Kraut, J. (1984) *J. Biol. Chem. 259*, 13027–13036.

Fishel, L. A., Villafranca, J. E., Mauro, J. M., & Kraut, J. (1987) *Biochemistry 26*, 351–360.

Fuchsman, W. M., & Appleby, C. A. (1979) *Biochemistry 28*, 1309–1321.

George, P., & Hanania, G. (1952) *Biochem. J. 52*, 517–523.

George, P., & Hanania, G. (1953) *Biochem. J. 55*, 236–243.

George, P., & Irvine, D. H. (1956) *J. Colloid Sci. 11*, 327–339.

Gersonde, K., Yu, N.-T., Lin, S.-H., Smith, K. M., & Parish, D. W. (1989) *Biochemistry 28*, 3960–3966.

Goodin, D. B., Mauk, A. G., & Smith, H. (1986) *Proc. Natl. Acad. Sci. U.S.A. 83*, 1295–1299.

Hashimoto, S., Teraoka, J., Inubishi, T., Yonetani, T., & Kitagawa, T. (1986a) *J. Biol. Chem. 261*, 11110–11118.

Hashimoto, S., Tatsuno, Y., & Kitagawa, T. (1986b) *Proc. Natl. Acad. Sci. U.S.A. 83*, 2417–2421.

Hildebrandt, P., Heimburg, T., & Marsh, D. (1990a) *Eur. Biophys. J. 18*, 193.

Hildebrandt, P., Heimburg, T., Marsh, D., & Powell, G. L. (1990b) *Biochemistry 29*, 1661–1668.

Iizuka, T., Makino, R., Ishimura, Y., & Yonetani, T. (1985) *J. Biol. Chem. 260*, 1407–1412.

Jongeward, K. A., Magde, D., Taube, D. J., & Traylor, T. G. (1988) *J. Biol. Chem. 263*, 6027–6030.

Kaput, J., Goltz, S., & Blobel, G. (1982) *J. Biol. Chem. 257*, 11186–11190.

Keilin, D., & Hartree, E. F. (1951) *Biochem. J. 49*, 88–97.

Kerr, E. R., & Yu, N.-T. (1988) in *Biological Applications of Raman Spectroscopy* (Spiro, T. G., Ed.) Vol. 3, pp 39–96, Wiley, New York.
Kimura, S., Yamazaki, I., & Kitagawa, T. (1981) *Biochemistry 20*, 4632–4638.
Li, X.-Y., & Spiro, T. G. (1988) *J. Am. Chem. Soc. 110*, 6024–6033.
Li, X.-Y., Czernuszewicz, R. S., Kinkaid, J. R., & Spiro, T. G. (1989) *J. Am. Chem. Soc. 111*, 7012–7023.
Li, X.-Y., Czernuszewicz, R. S., Kinkaid, J. R., Stein, P., & Spiro, T. G. (1990) *J. Phys. Chem. 94*, 47–61.
Loo, S., & Erman, J. E. (1975) *Biochemistry 14*, 3467–3470.
Miller, M. A., Hazzard, J. T., Mauro, J. M., Edwards, S. L., Simons, P. C., Tollin, G., & Kraut, J. (1988) *Biochemistry 27*, 9081–9088.
Miller, M. A., Coletta, M., Mauro, J. M., Putnam, L. D., Farnum, M. F., Kraut, J., & Traylor, T. G. (1990a) *Biochemistry 29*, 1777–1791.
Miller, M. A., Mauro, J. M., Smulevich, G., Coletta, M., Kraut, J., & Traylor, T. G. (1990b) *Biochemistry 29*, 9978–9988.
Paul, K. G., Theorell, H., & Akesson, A. (1953) *Acta Chem. Scand. 7*, 1284–1287.
Paul, J., Smith, M. L., & Paul, K.-G. (1985) *Biochim. Biophys. Acta 832*, 257–264.
Poulos, T. L., & Kraut, J. (1980a) *J. Biol. Chem. 255*, 8199–8205.
Poulos, T. L., & Kraut, J. (1980b) *J. Biol. Chem. 255*, 10322–10330.
Poulos, T. L., & Finzel, B. C. (1984) *Peptide and Proteins Review* (Hearn, M. T. W., Ed.) Vol. 4, pp 115–171, Marcel Dekker, New York.
Poulos, T. L., Freer, S. T., Alden, R. A., Edwards, S. L., Skogland, U., Takio, K., Eriksson, B., Xuong, N., Yonetani, T., & Kraut, J. (1980) *J. Biol. Chem. 255*, 575–580.
Ramsden, J., & Spiro, T. G. (1989) *Biochemistry 28*, 3125–3128.
Satterlee, J. D., & Erman, J. E. (1983) *J. Biol. Chem. 258*, 1050–1056.
Satterlee, J. D., Erman, J. E., Mauro, J. M., & Kraut, J. (1990) *Biochemistry 29*, 8797–8804.
Scholes, C. P., Liu, Y., Fishel, L. A., Farnum, M. F., Mauro, J. M., & Kraut, J. (1989) *Isr. J. Chem. 29*, 85–92.
Sitter, A. J., Reczek, C. M., & Terner, J. (1986) *J. Biol. Chem. 261*, 8638–8642.
Sitter, A. J., Shifflett, J. R., & Terner, J. (1988) *J. Biol. Chem. 263*, 13032–13038.
Sivaraja, M., Goodin, D. B., Mauk, A. G., Smith, M., & Hoffman, B. M. (1989) *Science 245*, 738–740.
Smulevich, G., Evangelista-Kirkup, R., English, A. M., & Spiro, T. G. (1986) *Biochemistry 25*, 4426–4430.
Smulevich, G., Mauro, J. M., Fishel, L. F., English, A. M., Kraut, J., & Spiro, T. G. (1988a) *Biochemistry 27*, 5477–5485.
Smulevich, G., Mauro, J. M., Fishel, L. F., English, A. M., Kraut, J., & Spiro, T. G. (1988b) *Biochemistry 27*, 5486–5492.
Smulevich, G., Miller, M. A., Gosztola, D., & Spiro, T. G. (1989a) *Biochemistry 28*, 3960–3966.
Smulevich, G., Mantini, A. R., English, A. M., & Mauro, J. M. (1989b) *Biochemistry 28*, 5058–5064.
Smulevich, G., Wang, Y., Edwards, S. L., Poulos, T. L., English, A. M., & Spiro, T. G. (1990a) *Biochemistry 29*, 2586–2592.
Smulevich, G., Wang, Y., Mauro, J. M., Wang, J., Fishel, L. A., Kraut, J., & Spiro, T. G. (1990b) *Biochemistry 29*, 7174–7180.
Spiro, T. G., Smulevich, G., & Su, C. (1990) *Biochemistry 29*, 4497–4508.
Strekas, T. C., & Spiro, T. G. (1974) *Biochim. Biophys. Acta 351*, 237–245.
Strittmatter, P., & Velick, S. F. (1956) *J. Biol. Chem. 221*, 253–264.
Su, Y. O., Czernuszewicz, R. S., Miller, L. A., & Spiro, T. G. (1988) *J. Am. Chem. Soc. 110*, 4150–4157.
Teraoka, J., & Kitagawa, T. (1981) *J. Biol. Chem. 256*, 3969–3977.
Teraoka, J., Job, D., Morita, Y., & Kitagawa, T. (1983) *Biochim. Biophys. Acta 747*, 10–15.
Terner, J., & Reed, D. E. (1984) *Biochim. Biophys. Acta 789*, 80–86.
Thanabal, V., de Ropp, J. S., & La Mar, G. N. (1988) *J. Am. Chem. Soc. 110*, 3027–3035.
Tsubaki, M., & Ichikawa, Y. (1985) *Biochim. Biophys. Acta 827*, 268–274.
Tsubaki, M., Srivastava, R. B., & Yu, N.-T. (1982) *Biochemistry 21*, 1132–1140.
Tsubaki, M., Hitawashi, A., & Ichekawa, Y. (1986) *Biochemistry 25*, 3563–3569.
Uno, T., Nishimura, Y., Tsuboi, M., Makino, R., Iizuka, T., & Ishimura, Y. (1987) *J. Biol. Chem. 262*, 4549–4556.
Vitello, L. B., Huang, M., & Erman, J. E. (1990a) *Biochemistry 29*, 4283–4288.
Vitello, L. B., Erman, J. E., Mauro, J. M., & Kraut, J. (1990b) *Biochim. Biophys. Acta 1038*, 90–97.
Wang, J., Mauro, J. M., Edwards, S. L., Oatley, S. L., Fishel, L. A., Ashford, V. A., Xuong, N.-H., & Kraut, J. (1990) *Biochemistry 29*, 7170–7173.
Williams, R. J. P. (1951) *Chem. Rev. 56*, 299–328.
Yonetani, T. (1976) *Enzymes, 3rd ed., 13*, 345–361.
Yonetani, T., & Anni, H. (1987) *J. Biol. Chem. 262*, 9547–9554.
Yonetani, T., Wilson, D. F., & Seamonds, B. (1966) *J. Biol. Chem. 241*, 5347–5352.